Sliding Mode Control in a Multi-loop Framework for Current Control of a Grid-tied Inverter via LCL-filter

Rodrigo Padilha Vieira*, Márcio Stefanello†, Rodrigo Varella Tambara* and Hilton Abílio Gründling*
* Federal University of Santa Maria - UFSM
Power Electronics and Control Research Group - GEPOC, Santa Maria, Brazil
† Federal University of Pampa - UNIPAMPA
Electronic Systems Research Group - GPSEl, Alegrete, Brazil
e-mail: rodrigovieira@ieee.org, marciostefanello@unipampa.edu.br, rodvarella10@gmail.com, ghilton03@gmail.com

***Abstract*—This paper proposes a current controller for grid tied Voltage Source Inverter (VSI) via a LCL filter using discrete-time Sliding Mode Control (SMC) in a multi-loop framework. The inner loop is implemented by the SMC with reference generated by an outer controller for the VSI side current. The tracking of the current entering the distribution network is ensured by a outer controller with a derivative + ressonant structure (for compensation and disturbance rejection with reference tracking). Simulation and experimental results are presented to validate the good performance of the proposed control strategy.**

***Keywords*—LCL filter, Sliding Mode Control, multi-loop control.**

I. Introduction

The widespread use of grid-tied converters for power processing in the last decades, boosted researches in the field of power electronics mainly applications such as in active filtering and Distributed Generation (DG). The majority of converters applied are of Voltage Source Inverter (VSI) type and, to the authors knowledge, most researches addresses DG applications. In this type of application, the VSI is interfaced with the grid via a LCL filter [1]. The benefits of this type of filter are well known. Among them, one can mention the switching harmonics attenuation, reduction of the reactive power consumption and the voltage drop from the converter to the point of common coupling with the grid. However, disadvantages make the problem of control a matter of concern. Due to this, most researches focuses on the development of controllers that meet with the requirements imposed by the system and on the application itself. More specifically, active damping [2], robustness with respect to grid impedance uncertainties [3]–[5] and reference tracking with disturbance rejection. The last one makes use of Proportional+Ressonant (PR) controllers in stationary $\alpha\beta$ frame [5]–[7] or Proportional+Integral (PI) controllers in rotating dq frame [8].

Thanks to the interaction between classical PI and PR controllers with the grid impedance [1], [9], several control approaches have been developed aiming to replace such kind of controllers or operate them in a combined manner. Among the alternative approaches, in [10] is proposed a Deadbeat controller with a real-time estimation of the unmodeled dynamics and the grid induced distortion. Thus, robustness and disturbance rejection capacity are addressed in the approach. An adaptive controller is applied for the current control in [4]. The main benefits are the inherent capacity of compensation of parametric uncertainties and robustness against unmodeled dynamics with a fast transient response. In this case, the disturbance compensation is carried out by an adaptive feedforward cancelation scheme.

In the previous approaches the disturbance rejection and reference tracking are achieved without the inclusion of PI or PR controllers. However, one has to mention other approaches that, even applying PI or PR controllers, proposes design methods or combination strategies to improve some characteristic of the system. As example, one has [5] that makes use of linear matrix inequalities to design a state feedback controller. The design is accomplished to ensure robustness for a known range of grid impedance values. The combination of controllers in a cascaded form is an alternative to the control of a LCL filter, giving rise to a multiloop control approach [11], [12]. In this type of controller, an outer loop is designed for reference tracking whilst the inner loop is designed for a fast dynamical response against disturbances and for improvement the system stability. The system performs better in terms of disturbance rejection and stability if using the inner variable as the one that responds faster to the disturbances.

The control approach presented in this paper follows the line proposed in [11]. In this case, the converter current is used as the inner variable to be controlled and a Sliding Mode Control (SMC) is the inner controller used to ensure a fast dynamical response. The choice for the SMC was motivated by its simplicity of implementation, disturbance rejection capacity and inherent robustness. In the literature these techniques are addressed for control and state estimation in several processes such as discussed in [13], [14], being implemented in digital processors [15], [16]. It will be demonstrated that the SMC allows the design of some closed-loop dynamics regardless of system parameters. However, the plant still presents an underdamped response and to improve the stability margin a Derivative controller is used in the outer loop. This controller is augmented with PR controllers for reference tracking with disturbance rejection.

This paper is organized as follows. In Section II, the model of the LCL filter and the control problem are formulated. The inner and outer control loops are presented in sections III and IV. Section V brings simulation results, some of which are used for comparison wit he the experimental results presented in Section VI. Finally, Section VII ends the paper with the conclusions.

978-1-4799-4032-5/14/$31.00 ©2014 IEEE

II. Plant Model and Multi-Loop Control

A. Model of the LCL filter

Several current control strategies for three-phase converters are carried out in stationary $\alpha\beta$ coordinates by means of a linear transformation over the three-phase system variables. For a balanced system, this linear transformation gives rise to two decoupled single-phase systems related with axis α and β. Due to this reason, for modeling and design, we consider the single-phase circuit presented in Fig. 1.

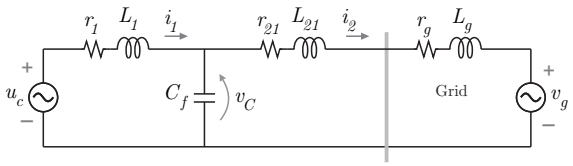

Figure 1. Single-phase circuit of a LCL filter.

By defining the resistance and inductance of the grid side as $r_2 = r_{21} + r_g$ and $L_2 = L_{21} + L_g$ respectively, and considering the states of the dynamic system as $\mathbf{x} = \begin{bmatrix} i_1 & v_C & i_2 \end{bmatrix}^T$, then the space state model $\dot{\mathbf{x}} = \mathbf{A}\mathbf{x} + \mathbf{B}u_c + \mathbf{G}v_g$, $y = \mathbf{C}\mathbf{x}$ for $y = i_1$ is given by

$$\begin{aligned} \begin{bmatrix} \dot{i}_1 \\ \dot{v}_C \\ \dot{i}_2 \end{bmatrix} &= \begin{bmatrix} -\frac{r_1}{L_1} & -\frac{1}{L_1} & 0 \\ \frac{1}{C_f} & 0 & -\frac{1}{C_f} \\ 0 & \frac{1}{L_2} & -\frac{r_2}{L_2} \end{bmatrix} \begin{bmatrix} i_1 \\ v_C \\ i_2 \end{bmatrix} + \\ &\quad \begin{bmatrix} \frac{1}{L_1} \\ 0 \\ 0 \end{bmatrix} u_c + \begin{bmatrix} 0 \\ 0 \\ -\frac{1}{L_2} \end{bmatrix} v_g, \\ i_1 &= \begin{bmatrix} 1 & 0 & 0 \end{bmatrix} \begin{bmatrix} i_1 \\ v_C \\ i_2 \end{bmatrix}. \end{aligned} \tag{1}$$

The model presented in (1) should also consider as output the current i_2. In this case, $y = \overline{\mathbf{C}}\mathbf{x}$, with $\overline{\mathbf{C}} = \begin{bmatrix} 0 & 0 & 1 \end{bmatrix}$.

By using the Euler method with a sampling period T_s, from (1) the following discrete-time state space equation can be obtained:

$$\begin{aligned} \begin{bmatrix} i_{1(k+1)} \\ v_{C(k+1)} \\ i_{2(k+1)} \end{bmatrix} &= \begin{bmatrix} 1-\frac{r_1}{L_1}T_s & -\frac{1}{L_1}T_s & 0 \\ \frac{1}{C_f}T_s & 1 & -\frac{1}{C_f}T_s \\ 0 & \frac{1}{L_2}T_s & 1-\frac{r_2}{L_2}T_s \end{bmatrix} \begin{bmatrix} i_{1(k)} \\ v_{C(k)} \\ i_{2(k)} \end{bmatrix} \\ &\quad + \begin{bmatrix} \frac{1}{L_1}T_s \\ 0 \\ 0 \end{bmatrix} u_{c(k)} - \begin{bmatrix} 0 \\ 0 \\ \frac{1}{L_2}T_s \end{bmatrix} v_{g(k)}. \end{aligned} \tag{2}$$

B. Multi-loop control strategy

The control of grid-tied power converters via LCL filter is a challenge due to the underdamped response and the presence of disturbances and parametric uncertainties associated with the electric grid. Thus, the controller must be properly chosen and designed to provide enough stability margins as well as robustness and tracking with disturbance rejection capacity.

Based on the above considerations, this paper proposes the multi-loop control topology depicted in Fig. 2. An outer control loop is implemented by a Derivative plus Resonant (denoted by D and R, respectively) controllers to provide the reference i_1^* for the converter side current. Thus, the task of the inner control loop is the tracking of the converter side current i_1 via a SMC.

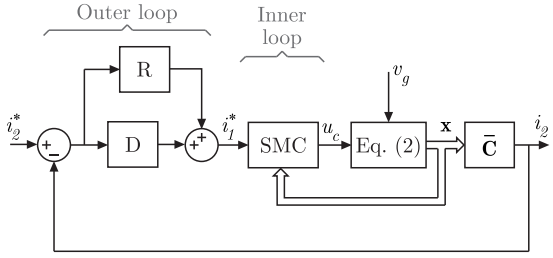

Figure 2. Block diagram of the proposed multi-loop control system. Inner loop with a SMC and outer loop with Derivative (D) plus Resonant (R) controllers for reference tracking and disturbance rejection.

The choice of the control system depicted in Fig. 2, particularly the inner loop based on the SMC, was motivated by the possibility of ensuring the fast tracking of the current i_1. Thus, a robust control system is ensured against unmodeled dynamics and disturbances.

III. Inner Loop: Sliding Mode Control

We now develop the control law that implements the SMC and find out the behavior of the inner controlled variable i_1. To perform these two tasks, one has to consider the overall control system depicted in Fig. 2 and the aim of the inner controller (SMC), i.e., the tracking of the current i_1. For this reason, lets define the sliding hyperplane

$$\sigma = i_1 - i_1^*. \tag{3}$$

Now, from (3) and (2) it is possible to obtain,

$$\begin{aligned} \sigma_{(k+1)} &= i_{1(k+1)} - i^*_{1(k+1)} \\ &= \left(1 - \frac{r_1}{L_1}T_s\right) i_{1(k)} - \frac{1}{L_1}T_s v_{C(k)} + \\ &\quad \frac{1}{L_1}T_s u_{c(k)} - i^*_{1(k+1)}. \end{aligned} \tag{4}$$

This paper makes use of the approach proposed in [16], which is given by the following reaching law for discrete-time systems:

$$\sigma_{(k+1)} - \sigma_{(k)} = -\varepsilon T_s \text{sign}\sigma_{(k)} - qT_s\sigma_{(k)}, \tag{5}$$

where ε and q are positive constants and sign denotes the signal function.

From (4) it is possible to obtain the following expression

$$\begin{aligned} \sigma_{(k+1)} - \sigma_{(k)} &= \left(1 - \frac{r_1}{L_1}T_s\right) i_{1(k)} - \frac{1}{L_1}T_s v_{C(k)} \\ &\quad + \frac{1}{L_1}T_s u_{c(k)} - i^*_{1(k+1)} \\ &\quad - \left(i_{1(k)} - i^*_{1(k)}\right). \end{aligned} \tag{6}$$

Then, combining (5) and (6) it is possible to design the control law

$$\begin{aligned} u_{c(k)} = &- \left(\frac{L_1}{T_s} - r_1\right) i_{1(k)} + v_{C(k)} + \frac{L_1}{T_s} i^*_{1(k+1)} \\ &+ \frac{L_1}{T_s}\left(i_{1(k)} - i^*_{1(k)}\right) \\ &- L_1 \varepsilon \text{sign}\left(\sigma_{(k)}\right) - L_1 q \sigma_{(k)}. \end{aligned} \tag{7}$$

One can verify that the control law u_c (7) is causal, its coefficients are independent of the grid side parameters (r_{21}, r_g, L_{21} and L_g) and the disturbance v_g (see Fig. 2) does not appear in the control law expression (7). Thus, the SMC ensures the decoupling of the inner control loop with respect to the grid voltage.

However, one can see from (7) that to compute $u_{c(k)}$ one need the value of $i^*_{1(k+1)}$. To solve this problem, $i^*_{1(k+1)}$ is replaced by its filtered value, $i^*_{1f_{(k+1)}}$ in order to make the control law causal. For this, the following transfer function is implemented:

$$\frac{I_{1f}}{I_1} = F(z) = \frac{1-p}{z-p}, \tag{8}$$

with $p \ll 1$. Then, by rewriting the control law given in (7) as

$$\begin{aligned} u_{c(k)} = &- \left(\frac{L_1}{T_s} - r_1\right) i_{1(k)} + v_{C(k)} + \frac{L_1}{T_s} i^*_{1f(k+1)} \\ &+ \frac{L_1}{T_s}\left(i_{1(k)} - i^*_{1(k)}\right) \\ &- L_1 \varepsilon \text{sign}\left(\sigma_{(k)}\right) - L_1 q \sigma_{(k)}, \end{aligned} \tag{9}$$

replacing this expression into (2) and neglecting the time delay of one sample associated with the digital implementation of the controller, the output i_1 of the plant is given by

$$\begin{aligned} i_{1(k+1)} = &\left(1 - \frac{r_1}{L_1} T_s\right) i_{1(k)} - \frac{1}{L_1} T_s v_{C(k)} \\ &- \left(1 - \frac{r_1}{L_1} T_s\right) i_{1(k)} + T_s q \sigma_{(k)} \\ &+ \frac{1}{L_1} T_s v_{C(k)} + {}^*_{1f(k+1)} + \left(i_{1(k)} - i^*_{1(k)}\right) \\ &- T_s \varepsilon \text{sign}\left(\sigma_{(k)}\right). \end{aligned} \tag{10}$$

By solving (10) one has

$$i_{1(k+1)} = i^*_{1f(k+1)} + (1 - T_s q)\,\sigma_{(k)} - T_s \varepsilon \text{sign}\left(\sigma_{(k)}\right). \tag{11}$$

The analysis of (11) points out also the reason for choosing i_1 as the inner control variable, the capacity of design its behavior by choosing the switching band of the SMC and the filter given in (8). One can note also the insensitiveness of the inner control loop with respect to the grid voltage v_g. Once the design of the inner loop is accomplished, the design of the outer loop for the tracking of i_2 with disturbance rejection is the next task. This topic is addressed in the next section.

IV. Outer loop: Derivative + Resonant Control

In this section it is developed the model for the inner closed loop system, which will allow us to design the outer controller.

From (11) and (8) it is possible to obtain

$$I_1 = G_{I_1^* \to I_1}(z)\, I_1^* - d(z), \tag{12}$$

where

$$G_{I_1^* \to I_1}(z) = \frac{(qT_s - p)\left(z + p\frac{1-qT_s}{qT_s-p}\right)}{(z-p)\,(z-(1-qT_s))} \text{ and}$$

$$d(z) = \frac{\varepsilon T_s}{z-(1-qT_s)} \text{sign}\sigma_{(k)}.$$

The above result was obtained without the delay related with the digital implementation. Thus, in the design of the outer loop, one has to consider one sample time of delay for the controller. Then, define

$$I_1 = G_1(z)\, I_1^* - d(z), \tag{13}$$

with $G_1(z) = G_{I_1^* \to I_1}(z)/z$.

Now, recall the diagram of Fig. 2 and the fact that the outer controlled variable is the grid side current i_2. Then, one can obtain the model relating this variable with the converter side current i_1. By neglecting the resistances, the following transfer function can be obtained:

$$\begin{aligned} G_2(z) = \frac{i_2(z)}{i_1(z)} = &\frac{L_1(1-K_2)}{L_1 + K_2(L_{21}+L_g)} \\ &\times \frac{z^2 - 2\frac{\cos(\omega_n T_s) - K_2}{1-K_2} z + 1}{z^2 - 2\frac{\cos(\omega_n T_s) + K_2 \frac{L_{21}+L_g}{L_1}}{1+K_2\frac{L_{21}+L_g}{L_1}} z + 1}, \end{aligned} \tag{14}$$

where $K_2 = \frac{\sin(\omega_n T_s)}{\omega_n T_s}$. The transfer function $G_2(z)$ reveals the undamped response. To provide some stability margin, the following Derivative controller is used

$$D(z) = K_D \frac{z-1}{z}. \tag{15}$$

Furthermore, one has to consider the effect of the disturbance as well as the need for reference tracking. To accomplish with these tasks, resonant controllers $C_{R1}(z) \ldots C_{Rn}(z)$ are used. A discrete-time resonant controller is given by

$$C_{Rn}(z) = K_{Rn} \frac{z^2 - z\cos(\omega_n T_s)}{z^2 - 2z\cos(\omega_n T_s) + 1}, \tag{16}$$

where K_{Rn} is the controller gain and ω_n is the angular frequency of the n-th frequency to be compensated. The design of the outer loop controllers is based on the Root Locus analysis.

The block diagram of the overall system is shown in Fig. 3.

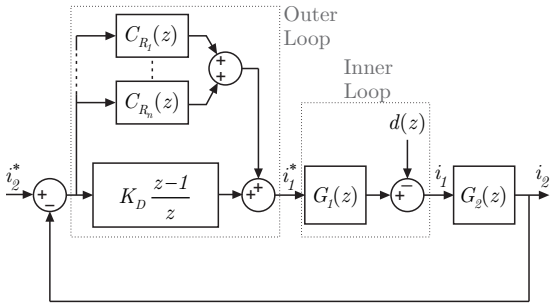

Figure 3. Block diagram of the proposed multi-loop control system.

V. Simulation Results

Simulation results were obtained aiming to evaluate the control strategy. The simulated system for the single-phase system is shown in Fig. 1 with the control structure given in Fig. 3. The simulation was performed in Matlab/Simulink® environment using a linear voltage source instead of a VSI. Despite this, some simulation results were obtained for the same conditions of the experimental system, thus demonstrating the good matching between the simulation and the experiment. Some parameters used in the simulation are summarized in Table I.

Table I. System parameters.

$L_1 = 1$ mH	$R_1 = 0.05\ \Omega$
$L_{21} = 0.5$ mH	$R_{21} = 0.05\ \Omega$
$C_f = 60\mu$F	$T_s = \frac{1}{12\times10^3}$ sec
SMC: $q = 10100,\ \epsilon = 700$	Filter $F(z)$: $p = 0.1$

The design of the SMC parameters was based on [16]. The design of the outer loop, in turn, was carried out from the Root Locus analysis of the system presented in Fig. 3, with the loop transfer function given by $G_1(z)\,G_2(z)\,(z-1)/z$.

Since $G_2(z)$ has dynamics dependent on the values of the grid parameters, some values for the the grid inductance L_g were evaluated for the design of the derivative gain K_D.

(i): The LCL filter has rated parameters and $L_g = 0$;

(ii): The LCL filter has rated parameters and $L_g = 5$mH;

(iii): The LCL filter has rated parameters and $L_g = 10$mH;

In terms of relative stability, the most critical case is associated with $L_g = 0$. In this case, the upper value for the derivative gain K_D for which the system remains stable is ≈ 0.9. In this paper we use $K_D = 0.4$, giving rise to a Gain Margin of 7.75dB and a Phase Margin of $14°$.

Now, one has to design the gain of the resonant controllers. For the tracking of i_2 it was used only the resonant controller $C_{R1}(z)$ (see (16)) for the fundamental frequency. The gain for this controller is obtained from the Root Locus analysis considering $L_g = 0$ in the loop transfer function of Fig. 3. From this analysis it was chosen $K_{R1} = 0.007082$, ensuring a stable closed-loop system.

The first simulation result was carried out aiming to verify the tracking of the i_1 and i_2 with the variation of the grid voltage. The grid voltage is $v_g(t) = 180\sin(\omega_1 t)$, with $\omega_1 = 2\pi60$rad/sec. At the time $t = 0.1$sec, the grid voltage changes to $v_g(t) = 311\sin(\omega_1 t)$. The grid reference current is set to $i_2^*(t) = 10\sin(\omega_1 t)$ in phase with the grid voltage v_g. Fig. 4 presents the first simulation result. This figure shows the good tracking of the i_1 and i_2 currents.

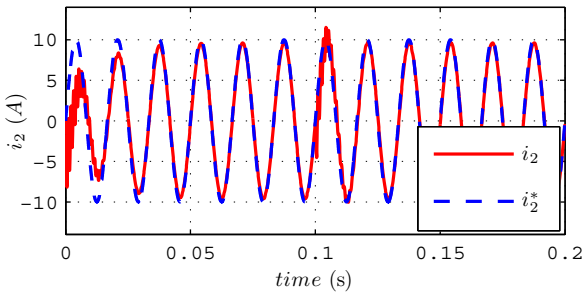

(a)

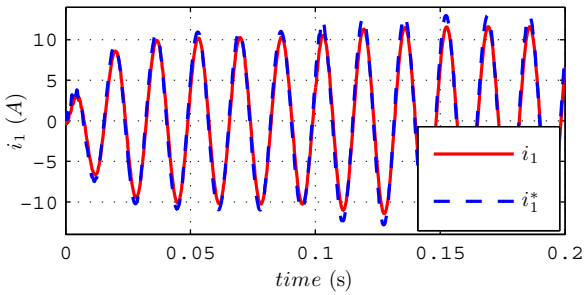

(b)

Figure 4. Simulations results with grid voltage variation. (a) i_2 and i_2^*. (b) i_1 and i_1^*.

.

The second set of simulations aims to demonstrate the performance under parameter uncertainties. To do this, the grid inductance L_g (see Fig. 1) of 2mH was added from the beginning of the simulation and bypassed at $t = 0.1$sec. Fig. 5 presents the results. One can verify that, despite the increase of 40% of the equivalent impedance at the grid side, the system still presents a good tracking performance.

Some simulation results were obtained to resemble the experiment. These simulation results are shown in Fig. 6. The test is carried out as follows: Starting with 0A, the reference current becomes $i_2^*(t) = 6\sin(2\pi60t)$ at $t = 0.1$sec. After 100ms, at $t = 0.2$ms, the amplitude of the reference current i_2^* is step changed from 6A to 10A. The good tracking performance of the grid current i_2 and the fast response of the inner controlled variable i_1 are verified in figures 6(a) and (b), respectively. The control action is shown in Fig. 6(c). It is worth nothing the good matching these results with the experimental ones presented in the next section, in Fig. 7.

VI. Experimental Results

Experimental results under similar conditions of the simulated ones presented in Section V were obtained to validate the proposed control method. The main difference lies in the fact that the experiment was carried out in absence of grid voltage, i.e, at short circuit condition. The control system was

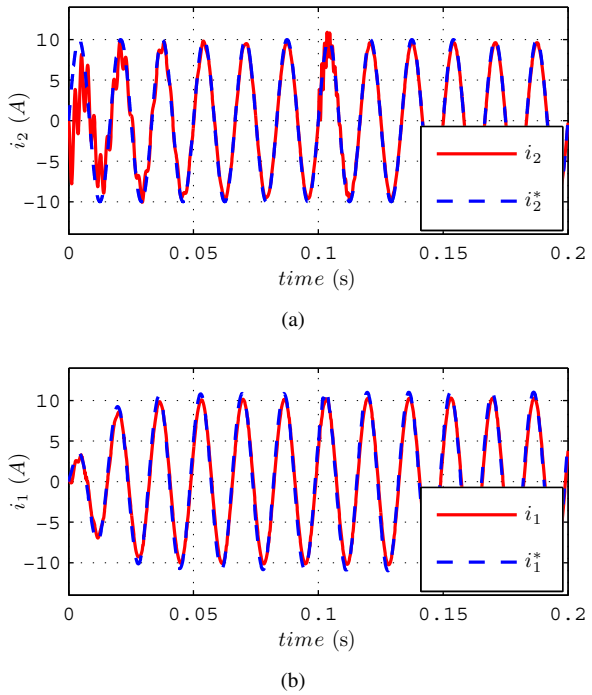

Figure 5. Simulation results with parameter uncertainties. (a) i_2 and i_2^*. (b) i_1 and i_1^*.

implemented in the floating point TMS320F28335 DSP and a three-phase inverter was used to modulated a three-level PWM waveform to synthesize the control action. The current control is carried out in $\alpha\beta$ axes. Thus, the three phase system is decoupled into two single-phase systems (α and β). The system parameters are given in Table I and the switching and sampling frequencies are set to the same value ($1/T_s$).

In order to validate the simulation, it is interesting to plot the electrical quantities presented in Fig. 6. For this, some experimental results are shown in Fig. 7 showing their compliance with the simulated ones. For plotting, the points were stored in a buffer into the DSP during the experiment. All the quantities are related with the α-axis. Figure 8 presents the three-phase currents at the grid side (i_2) obtained with the use of a oscilloscope.

VII. Conclusion

In this paper a discrete-time Sliding Mode Control (SMC) in a multi-loop framework is applied in the control of a VSI interfaced with the grid via a LCL-filter. The inner loop is used in the control of the converter current, whilst the tracking of the grid side current is ensured by resonant controllers. Besides the well-known robustness of the SMC, the approach allows to adjust the dynamics of the inner control loop almost independent of system parameters and the grid voltage. Thus, the design of the outer controller can be accomplished in a simple manner.

Acknowledgment

The authors would like to thank Coordenação de Aperfeiçoamento de Pessoal de Nível Superior (CAPES) for financial support.

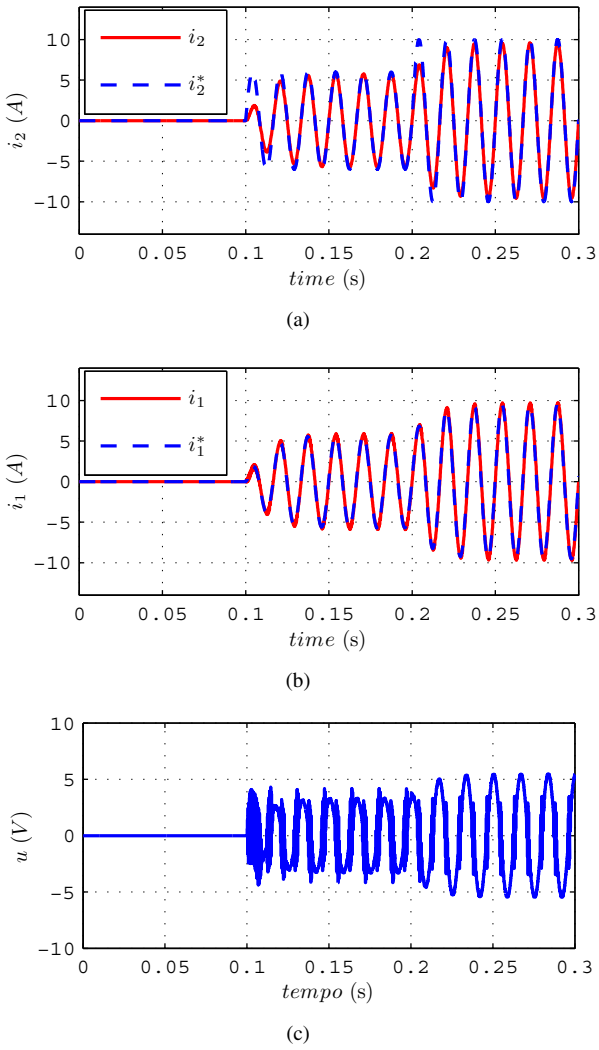

Figure 6. Simulation results with grid voltage variation. (a) i_2 and i_2^*. (b) i_1 and i_1^*. (c) Converter voltage.

References

[1] T. C. Wang, Z. Ye, G. Sinha, and X. Yuan, "Output Filter Design for a Grid-interconnected Three-phase Inverter," in *Proc. of IEEE 34th Annual Power Electronics Specialist Conference (PESC 03)*, 2003, pp. 779–784.

[2] F. Gervasio, R. Mastromauro, D. Ricchiuto, and M. Liserre, "Dynamic Analysis of Active Damping Methods for LCL-filter-based Grid Converters," in *Industrial Electronics Society, IECON 2013 - 39th Annual Conference of the IEEE*, Nov. 2013, pp. 671–676.

[3] M. Liserre, R. Teodorescu, and F. Blaabjerg, "Stability of Photovoltaic and Wind Turbine Grid-connected Inverters for a Large Set of Grid Impedance Values," *Power Electronics, IEEE Transactions on*, vol. 21, no. 1, pp. 263–272, Jan. 2006.

[4] J. Massing, M. Stefanello, H. Grundling, and H. Pinheiro, "Adaptive Current Control for Grid-Connected Converters With LCL Filter," *Industrial Electronics, IEEE Transactions on*, vol. 59, no. 12, pp. 4681–4693, Dec. 2012.

[5] L. Maccari, J. Massing, L. Schuch, C. Rech, H. Pinheiro, R. Oliveira, and V. Foletto Montagner, "LMI-Based Control for Grid-Connected Converters With LCL Filters Under Uncertain Parameters," *Power Electronics, IEEE Transactions on*, vol. 29, no. 7, pp. 3776–3785, July 2014.

[6] E. Twining and D. Holmes, "Grid Current Regulation of a Three-phase

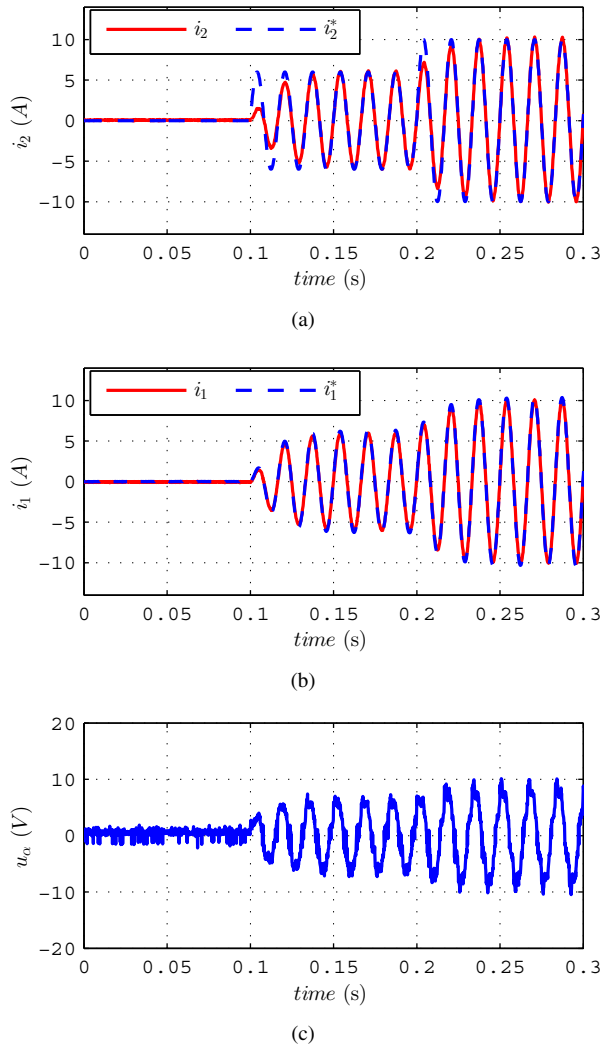

Figure 7. Experimental result. (a) i_2 e i_2^*. (b) i_1 e i_1^*. (c) Converter voltage.

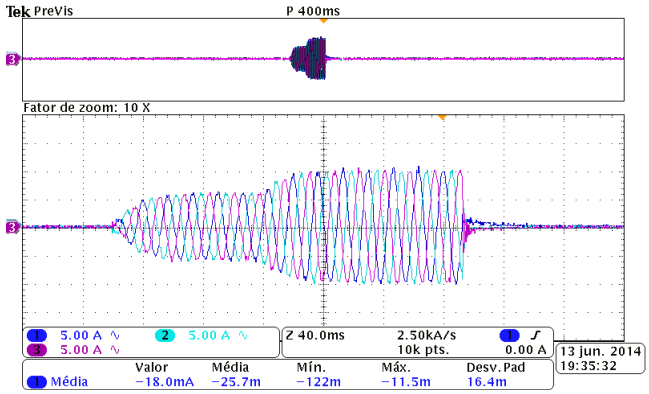

Figure 8. Grid side currents of the LCL filter.

Voltage Source Inverter with an LCL Input Filter," *Power Electronics, IEEE Transactions on*, vol. 18, no. 3, pp. 888–895, May 2003.

[7] G. Shen, X. Zhu, J. Zhang, and D. Xu, "A New Feedback Method for PR Current Control of LCL-Filter-Based Grid-Connected Inverter," *Industrial Electronics, IEEE Transactions on*, vol. 57, no. 6, pp. 2033–2041, Jun 2010.

[8] M. Liserre, F. Blaabjerg, and S. Hansen, "Design and Control of an LCL-filter-based Three-phase Active Rectifier," *Industry Applications, IEEE Transactions on*, vol. 41, no. 5, pp. 1281–1291, Sept 2005.

[9] J. Dannehl, C. Wessels, and F. Fuchs, "Limitations of Voltage-Oriented PI Current Control of Grid-Connected PWM Rectifiers with LCL Filters," *Industrial Electronics, IEEE Transactions on*, vol. 56, no. 2, pp. 380–388, Feb 2009.

[10] Y.-R. Mohamed, M. A-Rahman, and R. Seethapathy, "Robust Line-Voltage Sensorless Control and Synchronization of LCL -Filtered Distributed Generation Inverters for High Power Quality Grid Connection," *Power Electronics, IEEE Transactions on*, vol. 27, no. 1, pp. 87–98, Jan. 2012.

[11] P. C. Loh and D. Holmes, "Analysis of Multiloop Control Strategies for LC/CL/LCL-filtered Voltage-Source and Current-Source Inverters," *Industry Applications, IEEE Transactions on*, vol. 41, no. 2, pp. 644–654, March 2005.

[12] M. Durgante, H. Plotzki, and M. Stefanello, "Combined Active Damping with Adaptive Current Control for Converters with LCL filters," in *Industrial Electronics Society, IECON 2013 - 39th Annual Conference of the IEEE*, Nov 2013, pp. 520–525.

[13] A. Sabanovic, "Variable structure systems with sliding modes in motion control - a survey," *IEEE Transactions on Industrial Informatics*, vol. 7, no. 2, pp. 212 –223, May 2011.

[14] V. I. Utkin, J. Guldner, and J. Shi, *Sliding Mode Control in Electromechanical Systems*, 1st ed. Taylor & Francis, 1999.

[15] A. Bartoszewicz, "Discrete-time quasi-sliding-mode control strategies," *IEEE Transactions on Industrial Electronics*, vol. 45, no. 4, pp. 633 –637, Aug. 1998.

[16] W. Gao, Y. Wang, and A. Homaifa, "Discrete-time variable structure control systems," *IEEE Transactions on Industrial Electronics*, vol. 42, no. 2, pp. 117 –122, Apr. 1995.